

Enhancing Adversarial Training with Feature Separability

Yaxin Li Xiaorui Liu Han Xu Wentao Wang Jiliang Tang *

Abstract

Deep Neural Network (DNN) are vulnerable to adversarial attacks. As a countermeasure, adversarial training aims to achieve robustness based on the min-max optimization problem and it has shown to be one of the most effective defense strategies. However, in this work, we found that compared with natural training, adversarial training fails to learn better feature representations for either clean or adversarial samples, which can be one reason why adversarial training tends to have severe overfitting issues and less satisfied generalize performance. Specifically, we observe two major shortcomings of the features learned by existing adversarial training methods: (1) low intra-class feature similarity; and (2) conservative inter-classes feature variance. To overcome these shortcomings, we introduce a new concept of adversarial training graph (ATG) with which the proposed adversarial training with feature separability (ATFS) enables to coherently boost the intra-class feature similarity and increase inter-class feature variance. Through comprehensive experiments, we demonstrate that the proposed ATFS framework significantly improves both clean and robust performance. The implementation of this work can be found in the link¹.

1 Introduction

Although deep neural networks (DNNs) have achieved extraordinary accomplishments on various machine learning tasks, their vulnerability to adversarial attacks [1, 2] still raise great concerns when they are adopted to safety-critical tasks, such as autonomous vehicles [3] and AI healthcare [4]. As one of the most effective and reliable countermeasures to protect DNNs against adversarial attacks, adversarial training methods [5, 1, 6] train DNNs to correctly classify the manually generated adversarial examples around the clean samples. Particularly, they optimize the model to have the minimum adversarial risk of a perturbed adversarial sample.

However, adversarial training methods still suffer from major drawbacks in practice. For example, the

adversarially trained models always have lower clean accuracy than naturally trained models [7]. Furthermore, recent works [8, 9, 10] show that adversarially trained models have strong overfitting issues for adversarial robustness. In order to overcome these issues and improve the performance of adversarially trained models, some existing works attempt to leverage a much larger training set [8] or larger model architectures [11]. While, how to enhance adversarial training from algorithmic perspectives is still an open problem and requires deeper exploration.

In this work, we investigate potential reasons of the overfitting issues of adversarial training by examining the quality of their learned features. In our preliminary study, we observe that adversarial trained models always learn “unsatisfactory” features for both clean and adversarial samples. As an illustration, Figure 1 shows the learned features extracted from the second last layer of ResNet18 [12] models, which are trained by different algorithms on CIFAR10 [13] datasets, including natural training, PGD adversarial training [5], TRADES [6] and the AWP method [9]. The extracted features are visualized in a 2-dimensional space by t-SNE [14]. From Figure 1, we can make the following observations:

1. A naturally trained model can learn discriminative features for clean samples. Samples from different classes are well separated and the features of samples from the same class are well clustered. However, a naturally trained model cannot learn good features for the adversarial samples and the features of adversarial and clean samples are far away from each other. This can reflect the reason why naturally trained models can achieve high clean generalization but low robust performance.
2. For all adversarially trained models, including PGD training, TRADES and MART, the features of samples have much poorer “quality” than natural training. For example, for both clean or adversarial examples, (a) samples from the same class are not clustered together in the feature space; and (b) samples from different classes are not well separated. As a result, the trained models have poor ability to discriminate samples from different classes via the learned features. Thus, it could be one key

*Michigan State University. {liyaxin1, xiaorui, xuhan1, wangw116}@msu.edu

¹<https://github.com/no-name-submission/ATFS>

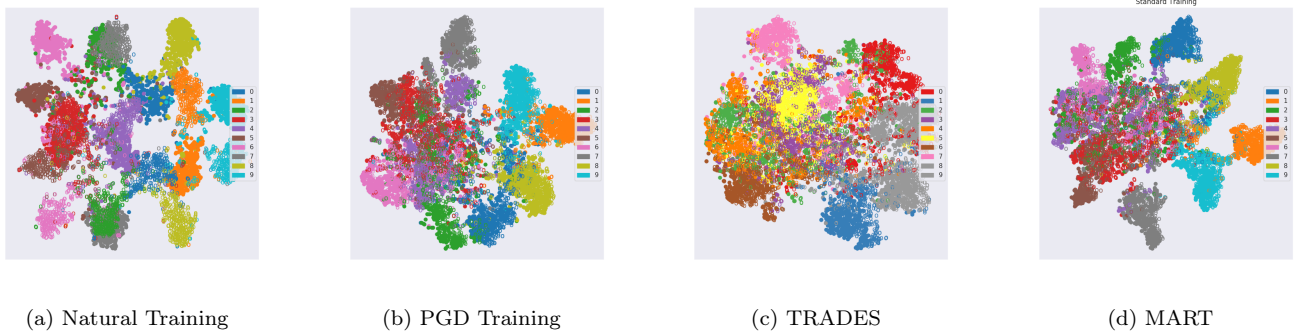


Figure 1: t-SNE feature visualization of naturally and adversarially trained models. The solid dots denote clean test samples and the hollow dots represent adversarial test samples generated by PGD-20 (8/255).

reason why the adversarially trained models suffer from both unsatisfactory clean accuracy & adversarial robustness.

These observations reveal two shortcomings of existing adversarial training methods. First, the inter-class feature variance is conservative. In other words, the model tends to embed samples from different classes with similar features. This makes the samples from different classes indistinguishable from each other and therefore degrades the clean classification performance and also contributes to unsatisfactory robustness. Second, low intra-class feature similarity results in a lack of clear clusters in the feature space. Therefore, the model can not easily extract the pattern for a specific class, which can degrade the clean performance. These shortcomings provide possible explanations for the phenomenon that adversarial training tends to have a large natural and robust generalization gap and can not achieve both high clean and robust performance.

Motivated by these findings, we aim to enhance adversarial training by mitigating the aforementioned shortcomings. We first introduce a novel concept of adversarial training graph (ATG) that can help encode various types of relations among clean and adversarial samples in adversarial training. By capturing the link information in ATG, the proposed adversarial training framework, ATFS, is facilitated to calibrate the learned features to render desired feature properties, including: (1) increasing intra-class feature similarity of both clean & adversarial examples, (2) increasing inter-class feature dissimilarity of both clean & adversarial examples, and (3) increasing feature similarity between each clean sample and its adversarial counterpart. Experimental results on benchmark datasets show that ATFS can achieve better performance than a variety of representative baselines. We also conduct experiments

to illustrate how ATFS mitigates the aforementioned shortcomings by feature visualization and boundary evaluation.

The remaining of the paper is organized as follows: in Section 2, we introduce the concept of ATG and the proposed ATFS framework in detail; in Section 3, we demonstrate the effectiveness of our model through empirical comparison with the state-of-art baselines and further ablation study; in Section 4, some related works are introduced; and in Section 5, we conclude this work and discuss future works.

2 The Proposed Framework

2.1 Notations Before we detail the proposed framework, we first introduce the necessary notations. In this paper, we consider the model is trained on the training set $\mathcal{D} = \{(\mathbf{x}_i, y_i)\}_{i=1}^n$, where \mathbf{x}_i is a clean training sample and $y_i \in \{1, \dots, C\}$ is the corresponding label with C being the number of classes. Correspondingly, $\{\mathbf{x}'_i\}_{i=1}^n$ represents the adversarial sample set generated from $\{\mathbf{x}_i\}_{i=1}^n$ by the current model f_θ . Note that an adversarial sample \mathbf{x}'_i is considered to have the same label y_i as its clean sample \mathbf{x}_i . As aforementioned, the adversarial training method and its variants minimize the model’s loss on the adversarial sample \mathbf{x}' which is computed by the inner maximization problem, which can be formulated as:

$$(2.1) \quad \min_{f_\theta} \max_{\|\mathbf{x}' - \mathbf{x}\|_p \leq \epsilon} \mathcal{L}(f_\theta(\mathbf{x}'), y).$$

Based on the discussion in Section 1, we found that adversarial training algorithms always tend to learn mixed features. Motivated by this finding, we propose the *Adversarial Training with Feature Separability* (ATFS) framework to calibrate the learned features for data samples that help achieve three major goals:

1. Increase intra-class feature similarity of both clean & adversarial examples,
2. Increase inter-class feature dissimilarity of both clean & adversarial examples
3. Increase feature similarity between each clean sample and its adversarial counterpart.

To achieve these goals, we first introduce *Adversarial Training Graph (ATG)* to encode the desired relations between training samples. In the following subsections, we will first introduce how to construct ATG for adversarial training. Then we detail the model components to capture different types of relations in ATG and consequently achieve the aforementioned goals. Finally, we present the final optimization objective and the proposed framework ATFS.

2.2 Adversarial Training Graph We formally define Adversarial Training Graph (ATG) as follows:

DEFINITION 2.1. (ADVERSARIAL TRAINING GRAPH)
An adversarial training graph $\mathcal{G} = \{\mathcal{V}, \mathcal{E}^+, \mathcal{E}^-\}$ is an undirected, weighted and sign graph with the node set $\mathcal{V} = \{\mathbf{x}_i\}_{i=1}^n \cup \{\mathbf{x}'_i\}_{i=1}^n$. ATG contains a set of positive links \mathcal{E}^+ and a set of negative links \mathcal{E}^- where \mathcal{E}^+ connects nodes from the same class while \mathcal{E}^- connects nodes from different classes.

In ATG, a positive link indicates that its two ending nodes are desired to be similar; while a negative link encourages dissimilarity between two nodes. In particular, to achieve the aforementioned three goals, we introduce three types of links in ATG as follows:

- **Positive links \mathcal{E}^+ .** All samples from the same class as sample \mathbf{x}_i are connected with \mathbf{x}_i by a positive link. In particular, we construct two types of positive links:
 - 1) \mathcal{E}_{ca}^+ : To enhance the robustness against adversarial samples, one strategy is to push clean samples close to their corresponding adversarial samples in the feature space such that the prediction for clean and adversarial samples are coherent and thus the model is less vulnerable to adversarial attacks. We achieve this by adding a positive link for each \mathbf{x}_i to its corresponding adversarial sample \mathbf{x}'_i in ATG. We denote this set of positive links as \mathcal{E}_{ca}^+ . Each edge connects a clean sample \mathbf{x}_i and its corresponding adversarial sample \mathbf{x}'_i with a link weight η_1 .
 - 2) \mathcal{E}_{intra}^+ : To boost intra-class feature similarity, one intuitive way is to enforce samples from the same class to be close in the feature space. Therefore, for a node \mathbf{x}_i with the label y_i , we connect it with all samples (including both clean and adversarial sample) from

the same class y_i excluding its adversarial sample. We denote this set of “intra-class” positive links, which is $\mathcal{E}^+ \setminus \mathcal{E}_{ca}^+$, as \mathcal{E}_{intra}^+ with a link weight η_2 .

- **Negative links \mathcal{E}^- .** To increase inter-class feature variance, we construct negative links between two nodes from different classes in ATG. We assign each negative link with a weight η_3 .

In ATG, we have two types of positive links which allows us to enforce different levels of similarity by controlling their link weights η_1 and η_2 . Meanwhile ATG is a complete graph which indicates that any pair of nodes in ATG is connected via either a positive link or a negative link. In the remaining of the paper, we use $\mathcal{E}_{ca}^+(i)$, $\mathcal{E}_{intra}^+(i)$ and $\mathcal{E}^-(i)$ to denote the three types of links for a node \mathbf{x}_i and define $\mathcal{E}(i)$ as $\mathcal{E}(i) = \mathcal{E}_{ca}^+(i) \cup \mathcal{E}_{intra}^+(i) \cup \mathcal{E}^-(i)$ to indicate all links connecting with \mathbf{x}_i . Suppose that we have a dataset with 5 samples $\{1, 2, 3, 4, 5\}$ from 2 classes $\{a, b\}$ where $\{1, 2, 3\} \in a$ and $\{4, 5\} \in b$. We use $\{1', 2', 3', 4', 5'\}$ to denote their corresponding adversarial samples. An illustration of links in ATG for this toy training dataset is demonstrated in Figure 2, where Figure 2a denotes positive links between clean samples and their corresponding adversarial samples, Figure 2b indicates positive links from the same class excluding \mathcal{E}_{ca}^+ and Figure 2c shows negative links. Note that for clarity, Figure 2c only shows negative links between the sample “1” from class a and samples from class b .

2.3 Capturing Link Information in ATG With the constructed ATG, the aforementioned three goals can be unified and simultaneously achieved by capturing link information in ATG. In general, ATG provides the guidance on the desired similarity of different samples around a center node \mathbf{x}_i . Specifically, we aim to maximize the representation similarity of samples connected by positive links and minimize the similarity of samples connected by negative links. Thus, we desire to learn a model with a representation function $h(\cdot)$ that has large $\mathcal{L}_{FS}(h, ATG, \mathbf{x}_i)$, which is defined as:

$$\begin{aligned} \mathcal{L}_{FS}(h, ATG, \mathbf{x}_i) = & \sum_{(\mathbf{x}_i, \mathbf{x}'_i) \in \mathcal{E}_{ca}^+(i)} s(h(\mathbf{x}_i), h(\mathbf{x}'_i)) \\ & + \sum_{(\mathbf{x}_i, \mathbf{x}_j) \in \mathcal{E}_{intra}^+(i)} s(h(\mathbf{x}_i), h(\mathbf{x}_j)) \\ & - \sum_{(\mathbf{x}_i, \mathbf{x}_j) \in \mathcal{E}^-(i)} s(h(\mathbf{x}_i), h(\mathbf{x}_j)), \end{aligned}$$

where $s(\cdot, \cdot)$ is a similarity function. By maximizing $\mathcal{L}_{FS}(h, ATG, \mathbf{x}_i)$ on the whole node set \mathcal{V} , we can achieve these goals on all samples. In this work, we define the

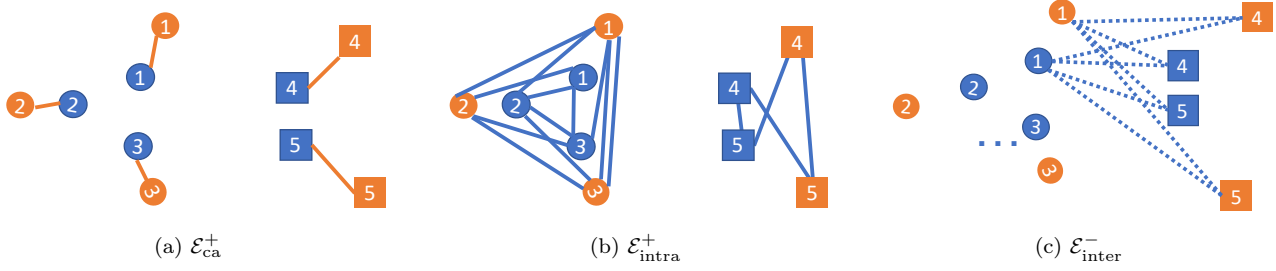


Figure 2: An illustration of links in ATG. We use blue and orange color to denote clean and adversarial samples respectively, and circles and squares to indicate classes a and b separately. The orange solid lines between adversarial samples are positive links in \mathcal{E}_{ca}^+ , the solid blue lines are positive links in \mathcal{E}_{intra}^+ , and the dotted lines are negative links in \mathcal{E}^- . Note that for clarity, we only show the negative links between the sample 1 from the class a to samples from the class b .

function $s(\cdot, \cdot, \cdot)$ in $\mathcal{L}_{FS}(h, ATG, \mathbf{x}_i)$ to measure the first-order proximity of a positive link in ATG. In particular, it is mathematically stated as the probability of the existence of a positive link among all links connected with the node \mathbf{x}_i , and modeled with a softmax function. Using a positive link $(\mathbf{x}_i, \mathbf{x}'_i) \in \mathcal{E}_{ca}^+(i)$ as an illustrative example, $s(h(\mathbf{x}_i), h(\mathbf{x}'_i))$ is defined as

$$(2.2) \quad s(h(\mathbf{x}_i), h(\mathbf{x}'_i)) = \frac{\exp(h(\mathbf{x}_i)^T h(\mathbf{x}'_i))}{S},$$

where

$$\begin{aligned} S = & \sum_{(\mathbf{x}_i, \mathbf{x}'_i) \in \mathcal{E}_{ca}^+(i)} \exp(h(\mathbf{x}_i)^T h(\mathbf{x}'_i)) \\ & + \sum_{(\mathbf{x}_i, \mathbf{x}_j) \in \mathcal{E}_{intra}^+(i)} \exp(h(\mathbf{x}_i)^T h(\mathbf{x}_j)) \\ & + \sum_{(\mathbf{x}_i, \mathbf{x}_j) \in \mathcal{E}^-(i)} \exp(h(\mathbf{x}_i)^T h(\mathbf{x}_j)). \end{aligned}$$

Given that the representation $h(\mathbf{x}_i)$ is normalized, $h(\mathbf{x}_i)^T h(\mathbf{x}'_i)$ essentially denotes the cosine similarity of $h(\mathbf{x}_i)$ and $h(\mathbf{x}'_i)$. Thus maximizing $s(h(\mathbf{x}_i), h(\mathbf{x}'_i))$ can naturally enforce large similarity between $h(\mathbf{x}_i)$ and $h(\mathbf{x}'_i)$. S is a normalization term over all links connecting to \mathbf{x}_i . With the definition of $s(\cdot, \cdot)$, $\mathcal{L}_{FS}(h, ATG, \mathbf{x}_i)$ can be rewritten as

$$(2.3) \quad \mathcal{L}_{FS}(h, ATG, \mathbf{x}_i) = \frac{1}{S} \left(\sum_{(\mathbf{x}_i, \mathbf{x}'_i) \in \mathcal{E}_{ca}^+(i)} \exp(h(\mathbf{x}_i)^T h(\mathbf{x}'_i)) + \sum_{(\mathbf{x}_i, \mathbf{x}_j) \in \mathcal{E}_{intra}^+(i)} \exp(h(\mathbf{x}_i)^T h(\mathbf{x}_j)) - \sum_{(\mathbf{x}_i, \mathbf{x}_j) \in \mathcal{E}^-(i)} \exp(h(\mathbf{x}_i)^T h(\mathbf{x}_j)) \right).$$

Note that the normalization denominator S is the summation of the numerators of the three terms in Eq. (2.3). Thus, one advantage of defining $s(\cdot, \cdot, \cdot)$ as Eq. (2.2) is – maximizing the first two terms for positive links in Eq. (2.3) will lead to minimizing the third term for negative links automatically. Therefore, we can further simplify $\mathcal{L}_{FS}(h, ATG, \mathbf{x}_i)$ in Eq. (2.3) as the mean of log-likelihood of all positive links connected by \mathbf{x}_i and add different weights to different types of links. Since different nodes in ATG can have different numbers of positive links, we add a normalization term $\frac{1}{|\mathcal{E}^+(i)|}$ in $\mathcal{L}_{FS}(h, ATG, \mathbf{x}_i)$. As a result, the feature separability loss is defined as follows:

$$(2.4) \quad \mathcal{L}_{FS}(h, ATG, \mathbf{x}_i) = \frac{1}{|\mathcal{E}^+(i)|} \left(\eta_1 \cdot \sum_{(\mathbf{x}_i, \mathbf{x}'_i) \in \mathcal{E}_{ca}^+(i)} \log \frac{\exp(h(\mathbf{x}_i)^T h(\mathbf{x}'_i))}{S} + \eta_2 \cdot \sum_{(\mathbf{x}_i, \mathbf{x}_j) \in \mathcal{E}_{intra}^+(i)} \log \frac{\exp(h(\mathbf{x}_i)^T h(\mathbf{x}_j))}{S} \right),$$

2.4 The ATFS Algorithm The final objective function for Adversarial Training with Feature Separability (ATFS) is a combination of the cross-entropy loss and the objective provided by ATG:

$$(2.5) \quad \min_{f_\theta} \sum_{x_i \in \mathcal{D}} \alpha \cdot \mathcal{L}_{adv}(f(\mathbf{x}'_i), y_i) - \sum_{x_i \in \mathcal{V}} \beta \cdot \mathcal{L}_{FS}(F(\cdot), ATG, \mathbf{x}_i),$$

where $F(\cdot)$ denotes the features extracted by the model, which is the output of the second last layer of the model. The first term in Eq. (2.5) is the cross-entropy

loss, which minimizes the error risk for the adversarial samples towards the correct labels. Here we have the flexibility to calculate \mathcal{L}_{adv} based on different adversarial training algorithm. The second term is the Feature Separability Loss which facilitates the model to learn separable feature representations. Two parameters α and β are predefined to balance the contributions from these two terms. In this work, we adopt SGD to optimize the proposed objective function. The detailed training algorithm for ATFS can be found in Appendix A.

3 Experiment

In this section, we conduct comprehensive experiments to evaluate the effectiveness of the proposed ATFS framework. We first introduce the experimental settings and then compare ATFS with representative baselines in terms of clean and robust performance. Next we conduct ablation study to show the impact of model components on ATFS and finally further probe the advantages of ATFS.

3.1 Experimental Settings In this section, we introduce the experimental setting including the details of the training and test phase.

Training Setup To demonstrate the effectiveness of the proposed framework, we conduct experiments on two model architectures, including ResNet18 [12] and WRN-34 [15]. We test the performance on two benchmark datasets, including CIFAR10 [13] and SVHN [16]. For CIFAR10, we use 49,000 images for training and the rest 1,000 images for validation. For SVHN, we use 72,257 images for training and 1,000 for validation. We train each model for a maximum of 120 epochs. While, recent study [10] suggests using early stopping because adversarial training suffers from serious overfitting issues. Therefore, we split the training set into a training set and a validation set, and use the validation set to select the best model for all experiments and baselines. All the models are trained using SGD with momentum 0.9, weight decay 2×10^{-4} and an initial learning rate of 0.1, which is divided by 10 at the 75-th and 90-th epoch. For the parameter selection, we set the weight β for the \mathcal{L}_{adv} as 1 and select the weight α for FS loss from $\{0.01, 0.05, 0.1, 0.2, 0.5\}$. Meanwhile, for the parameters in the ATG, we set $\eta_2 = \eta_3 = 1$ and keep η_1 flexible to ease the tuning process for our model. The adversarial samples used in training are calculated by PGD-10, with a perturbation budget $\epsilon = 8/255$, step size $\gamma = 2/255$ and step 10.

Robust Evaluation For robustness evaluation, we report robust accuracy under l_∞ -norm $8/255$ attacks generated by various attacking algorithms including FGSM attack [1], PGD attack [5], CW Attack optimized

with PGD [2] and Autoattack (AA) [17]. Note that AA is one of the strongest attack algorithms that ensembles three white-box attacks (APGD-CE, APGD-DLR, FAB) and one black-box attack (Square Attack). These attack methods are based on the implementation by DeepRobust [18] and Autoattack [17].

3.2 Robust Performance Comparison To assess the robustness achieved by ATFS, we compare the performance of ATFS with four adversarial training methods, including standard adversarial training (AT) [5], TRADES [6] and MART [19]. Two self-supervised related adversarial training methods SS-OOD (AT + Auxiliary Rotation) [20] and RoCL [21].

Performance Comparison on ResNet18 Table 1 shows the performance comparison on the CIFAR10 dataset and we can make the following observations. First, ATFS outperforms two classic adversarial training methods (AT and TRADES). For instance, in terms of Autoattack, the robust accuracy of ATFS improves over AT and TRADES ($1/\lambda = 5.0$) by 1.7% and 0.71% respectively, while maintaining similar or better clean accuracy. Note that TRADES also explores the relations among clean and adversarial samples, while ATFS explores not only the relationship between clean and adversarial samples but also the class wise relations via ATG. This comparison indicates that capturing the relations of inter and intra class samples can boost both the clean and robust performance. ATFS also significantly outperforms two self-supervised related adversarial training methods. In terms of PGD-20 attack, the robust accuracy of AT+ATFS improves over RoCL (AT finetune) and SS-OOD by 10.22% and 2.35%, respectively. When advanced adversarial training algorithms like TRADES and MART are combined with ATFS, the performance can be further improved. In principle, those methods improve adversarial training in different ways from ATFS and their contributions could be complementary. Therefore, a combination of them has the potential to further boost performance.

The performance comparison on the SVHN dataset is shown in Table 2 and we can make similar observations as those on the CIFAR10 dataset: AT+ATFS achieves better clean and robust performance than AT and TRADES in most of the cases. It also outperforms the self-supervised baseline SS-OOD by 7.41% under the PGD-20 attack. To combine with MART and TRADES, the performance is further improved. The combination of AT, TRADES, and MART is improved by 1.82%, 1.79% and 1.2% compared to the original algorithm.

Performance on WRN-34-10. To test the performance of ATFS with larger model capacity, we train it on WideResNet-34 [15] and we have similar observa-

Table 1: Performance Comparison on CIFAR10 with ResNet18.

	Clean	FGSM	PGD-20(8/255)	CW _{inf} (8/255)	AA(8/255)
AT	84.27	62.66±0.07	49.44±0.03	48.18±0.00	46.30
TRADES (1/λ = 5.0)	81.64	61.78±0.03	50.55±0.03	48.41±0.03	47.95
RoCL+AT (finetune)	80.26	58.14±0.00	40.77±0.00	40.12±0.00	40.12
SS-OOD	80.58	61.21±0.03	49.64±0.03	48.54±0.00	46.67
MART	83.07	65.43±0.07	53.25±0.03	49.46±0.00	47.93
AT+ATFS	83.74	64.64±0.03	51.99±0.00	53.02±0.00	48.03
TRADES + ATFS	81.88	63.26±0.03	52.24±0.00	49.72±0.05	48.66
MART + ATFS	82.79	64.00±0.00	54.50±0.00	50.12±0.00	48.39

Table 2: Performance Comparison on SVHN with ResNet18.

	Clean	FGSM	PGD-20(8/255)	CW _{inf} (8/255)	AA(8/255)
AT	91.49	63.38±0.00	52.71±0.00	48.64±0.00	44.07
TRADES (1/λ = 2.0)	90.84	71.09±0.03	54.79±0.03	51.24±0.00	47.36
TRADES (1/λ = 5.0)	89.82	71.97±0.00	56.83±0.03	52.83±0.00	48.14
SS-OOD	90.62	69.28±0.00	51.45±0.00	47.75±0.03	44.76
MART	92.02	74.41±0.03	57.76±0.03	51.18±0.03	47.20
AT + ATFS	89.95	72.79±0.07	58.82±0.00	52.77±0.04	45.89
TRADES + ATFS	90.30	73.55±0.02	58.86±0.02	54.35±0.04	49.93
MART + ATFS	91.79	74.17±0.01	57.25±0.02	51.06±0.00	48.40

tions with ResNet18: Adversarial training algorithms can achieve better performance with feature separability. The results can be found at Table 4 in Appendix B.

3.3 Ablation Study In this subsection, we aim to provide analysis on why ATFS can help both clean and robust performance. In particular, we study how the model components affect the performance of ATFS.

3.3.1 Effect of the FS Loss The training objective defined in Eq. (2.5) is the combination of the adversarial loss \mathcal{L}_{adv} and the proposed FS loss \mathcal{L}_{FS} . To study how \mathcal{L}_{FS} impacts the performance, we conduct experiments to see how the performance changes with the weight for \mathcal{L}_{FS} . We fix the weight parameter $\alpha = 1$ and changes β from 0.05, 0.1, 0.5, 1.0. The results on CIFAR10 is shown in Figure 3a.

In this figure, the red lines denote the clean performance and blue lines indicate the robust performance. We can observe that with the increase of the weight for \mathcal{L}_{FS} , the robust performance increases 4.2% compared to standard adversarial training ($\beta = 0$) on CIFAR10 while we do not observe an obvious decrease for clean accuracy. This is consistent with the result in SVHN dataset.

3.3.2 Effect of Adversarial Link Weight in ATG In ATG, we have two types of positive links, \mathcal{E}_{ca}^+ and

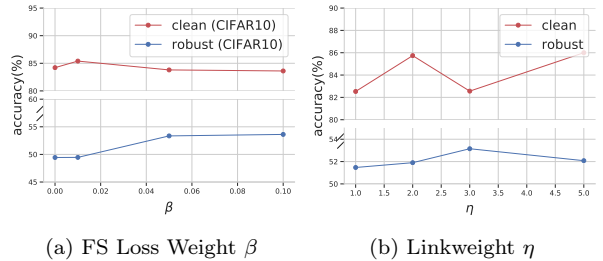


Figure 3: The impact of the FS loss and adversarial link weight

\mathcal{E}_{intra}^+ . Those two types of links are assigned with weights η_1 and η_2 , separately. We show how the robust performance changes along with the η_1 changes in Figure 3b. We can see that when the link weight between clean samples and adversarial samples grow slightly larger, the robust performance will increase since the model focuses more on robust performance. While if η_1 increases even larger, it would degrade the performance since it will reduce the effect of feature separability. It shows that the feature separability loss will actually contribute to the final robust performance.

3.4 Further Probing on Feature Space of ATFS In this subsection, we further probe the learned features

to demonstrate the advantages of ATFS by visualizing these features and measuring the boundary thickness.

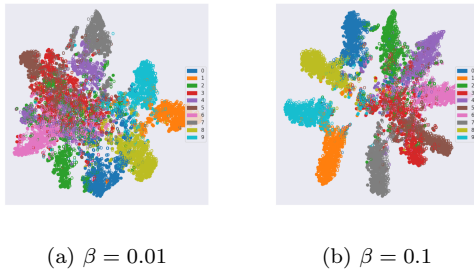


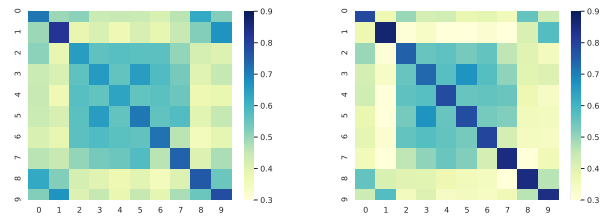
Figure 4: Features learned by PGD adversarial training and ATFS where Figure 4a shows the t-SNE feature visualization for the standard PGD adversarially trained model and Figure 4b illustrates the feature visualization for the model trained by ATFS.

3.4.1 Visualizing Learned Features To give an illustration of how the FS loss term affects the feature space of the trained model, we show 1) t-SNE visualization of learned features and 2) feature similarity heatmap among different classes.

Figure 4a and Figure 4b show the t-SNE feature visualization of standard adversarially trained model and the model trained by the ATFS framework when $\beta = 0.01$ and $\beta = 0.1$, respectively. For ATFS, representations of samples from different classes are well separated. Especially, clean samples and their corresponding adversarial samples in ATFS are closer to each other than AT. It demonstrates that, with the FS loss term, the objective can learn much better features and thus can explain why ATFS achieves good performance on both clean and robust samples.

In addition to visualizing learned features, we also examine the average feature similarity for samples among different classes. As shown in Figure 5, the value in the i -th row and the j -th column denotes the average feature similarity of samples from classes i and j , and darker color indicates higher similarity. Compared to standard adversarial training showed in Figure 5a, the value on the diagonal of the Figure 5b is larger, which suggests larger intra-class feature similarity for the model trained by the ATFS framework. On the other hand, the rest part of Figure 5b is lighter than Figure 5a, which indicates larger inter-class feature variance. To summarize, both the feature visualization and feature similarity verify that ATFS has achieved the aforementioned three goals and demonstrate why ATFS can achieve better performance.

3.4.2 Measuring Boundary Thickness Boundary thickness (BT) [22] is a robustness measurement that intuitively indicates the cost of generating adversarial



(a) Feature correlation for AT (b) Feature correlation for ATFS

Figure 5: Feature similarity heatmap for the standard adversarial training and ATFS.

samples for a model. Basically, the boundary thickness of a classifier measures the expected distance to travel along with line segments between different classes across a decision boundary. It has been proven that a larger boundary thickness is necessary for robust models [22]. Therefore, we calculate the boundary thickness for different robust models to compare their robustness properties. The result is summarized in Table 3. We can observe that ATFS has the largest thickness value, This observation is consistent with the previous observations that ATFS can achieve the best robust performance.

4 Related Work

Adversarial Attacks and Defenses The existence of several successful attack methods, such as fast gradient sign method (FGSM) [1], CW attack [2] and Projected Gradient Descent (PDG) attack [5], demonstrated the vulnerability of deep neural networks to adversarial samples. To improve the model robustness against adversarial samples, many defensive methods have been proposed including input denoising [23, 24], defensive distillation [25], gradient regularization [26, 23], adversarial training [5, 1] and certified defenses. Among them, adversarial training has been shown to be one of the most effective defenses [27]. Based on adversarial training, a number of variants have been developed to further improve the performance, including TRADES [6], MART [19], MMA training [28], FAT [29], GAIRAT [30]. Even though adversarial training and its variants are effective to improve model robustness, the adversarial training based methods still have several main drawbacks, such as the trade-off between clean accuracy and robust accuracy, which is first claimed in [6]; bad clean performance generalization [8] and robustness generalization [10], introducing fairness issue. Our work belongs to adversarial training method and we focus on a observed drawback of adversarial training, that is the learned feature is not well separated in feature space and thus lead to bad generalization.

Table 3: Measuring Boundary Thickness.

Method	AT	TRADES(2.0)	TRADES(5.0)	MART	ATFS
BT	2.21	2.51	3.04	2.60	3.23

Self-supervised Learning We mention that self-supervised learning techniques, such as Contrastive Learning methods [31] as another main category of related studies to this work. It is because these self-supervised learning techniques are also devised to extract high-quality representations, even in scenarios without any label information [32, 33]. By designing various pretext learning tasks, such as predicting the position of image patches [34] or classifying image rotation angles [35], self-supervised learning techniques guide the representation learning process on unlabeled examples in a supervised way. Particularly, some recent works also incorporate self-supervised learning techniques into supervised learning tasks [36, 37]. However, these techniques cannot be directly adopted into the adversarial learning setting.

Self-supervised Learning and Contrastive Learning Recent work shows that using additional unlabeled data could help model obtain robust representations; Another categorized of adversarial training variants are proposed to enhance adversarial training performance with self-supervised learning. For example, SS-OOD [20] arguments the adversarial data with different rotation angles. An auxiliary head network is added to the network to predict the angle and this self-supervised loss is utilized to help robust training.

5 Conclusion

In this work, we propose a novel Adversarial Training framework with Feature Separability (ATFS) to enhance adversarial training. Compared to previous adversarial training methods, ATFS utilizes ATG to capture various types of relations among adversarial and clean examples in adversarial training. As a result, ATFS learns better features for both clean and adversarial samples. Meanwhile, ATFS can achieve both better clean and robust accuracy compared to numerous representative baselines. We conducted comprehensive experiments to show the effectiveness of ATFS and try to understand the reason of ATFS could achieve good performance. In the future, we plan to try if ATFS can be applied to solve other problems in adversarial training, for example, data bias and adversarial training towards multiple bounds attack.

References

- [1] Ian J Goodfellow, Jonathon Shlens, and Christian Szegedy. Explaining and harnessing adversarial examples. *arXiv preprint arXiv:1412.6572*, 2014.
- [2] Nicholas Carlini and David Wagner. Towards evaluating the robustness of neural networks. In *2017 IEEE Symposium on Security and Privacy (SP)*, pages 39–57. IEEE, 2017.
- [3] Mariusz Bojarski, Davide Del Testa, Daniel Dworakowski, Bernhard Firner, Beat Flepp, Praseoon Goyal, Lawrence D Jackel, Mathew Monfort, Urs Muller, Jiakai Zhang, et al. End to end learning for self-driving cars. *arXiv preprint arXiv:1604.07316*, 2016.
- [4] Andre Esteva, Alexandre Robicquet, Bharath Ramsundar, Volodymyr Kuleshov, Mark DePristo, Katherine Chou, Claire Cui, Greg Corrado, Sebastian Thrun, and Jeff Dean. A guide to deep learning in healthcare. *Nature medicine*, 25(1):24–29, 2019.
- [5] Aleksander Madry, Aleksandar Makelov, Ludwig Schmidt, Dimitris Tsipras, and Adrian Vladu. Towards deep learning models resistant to adversarial attacks. *arXiv preprint arXiv:1706.06083*, 2017.
- [6] Hongyang Zhang, Yaodong Yu, Jiantao Jiao, Eric Xing, Laurent El Ghaoui, and Michael Jordan. Theoretically principled trade-off between robustness and accuracy. In *International Conference on Machine Learning*, pages 7472–7482. PMLR, 2019.
- [7] Dimitris Tsipras, Shibani Santurkar, Logan Engstrom, Alexander Turner, and Aleksander Madry. Robustness may be at odds with accuracy. *arXiv preprint arXiv:1805.12152*, 2018.
- [8] Ludwig Schmidt, Shibani Santurkar, Dimitris Tsipras, Kunal Talwar, and Aleksander Madry. Adversarially robust generalization requires more data. *arXiv preprint arXiv:1804.11285*, 2018.
- [9] Dongxian Wu, Shu-Tao Xia, and Yisen Wang. Adversarial weight perturbation helps robust generalization. *Advances in Neural Information Processing Systems*, 33, 2020.
- [10] Leslie Rice, Eric Wong, and Zico Kolter. Overfitting in adversarially robust deep learning. In *International Conference on Machine Learning*, pages 8093–8104. PMLR, 2020.
- [11] Guy Katz, Clark Barrett, David L Dill, Kyle Julian, and Mykel J Kochenderfer. Towards proving the adversarial robustness of deep neural networks. *arXiv preprint arXiv:1709.02802*, 2017.
- [12] Kaiming He, Xiangyu Zhang, Shaoqing Ren, and Jian Sun. Deep residual learning for image recognition. In *Proceedings of the IEEE conference on computer vision and pattern recognition*, pages 770–778, 2016.

- [13] Alex Krizhevsky, Geoffrey Hinton, et al. Learning multiple layers of features from tiny images. 2009.
- [14] Laurens Van der Maaten and Geoffrey Hinton. Visualizing data using t-sne. *Journal of machine learning research*, 9(11), 2008.
- [15] Sergey Zagoruyko and Nikos Komodakis. Wide residual networks. *arXiv preprint arXiv:1605.07146*, 2016.
- [16] Yuval Netzer, Tao Wang, Adam Coates, Alessandro Bissacco, Bo Wu, and Andrew Y Ng. Reading digits in natural images with unsupervised feature learning. 2011.
- [17] Francesco Croce and Matthias Hein. Reliable evaluation of adversarial robustness with an ensemble of diverse parameter-free attacks. In *International Conference on Machine Learning*, pages 2206–2216. PMLR, 2020.
- [18] Yaxin Li, Wei Jin, Han Xu, and Jiliang Tang. Deep-robust: A pytorch library for adversarial attacks and defenses. *arXiv preprint arXiv:2005.06149*, 2020.
- [19] Yisen Wang, Difan Zou, Jinfeng Yi, James Bailey, Xingjun Ma, and Quanquan Gu. Improving adversarial robustness requires revisiting misclassified examples. In *International Conference on Learning Representations*, 2019.
- [20] Dan Hendrycks, Mantas Mazeika, Saurav Kadavath, and Dawn Song. Using self-supervised learning can improve model robustness and uncertainty. *arXiv preprint arXiv:1906.12340*, 2019.
- [21] Minseon Kim, Jihoon Tack, and Sung Ju Hwang. Adversarial self-supervised contrastive learning. *arXiv, (NeurIPS):1–17*, 2020.
- [22] Yaoqing Yang, Rajiv Khanna, Yaodong Yu, Amir Gholami, Kurt Keutzer, Joseph E Gonzalez, Kannan Ramchandran, and Michael W Mahoney. Boundary thickness and robustness in learning models. *arXiv preprint arXiv:2007.05086*, 2020.
- [23] Florian Tramèr, Alexey Kurakin, Nicolas Papernot, Ian Goodfellow, Dan Boneh, and Patrick McDaniel. Ensemble adversarial training: Attacks and defenses. *arXiv preprint arXiv:1705.07204*, 2017.
- [24] Han Xu, Yao Ma, Hao-Chen Liu, Debayan Deb, Hui Liu, Ji-Liang Tang, and Anil K Jain. Adversarial attacks and defenses in images, graphs and text: A review. *International Journal of Automation and Computing*, 17(2):151–178, 2020.
- [25] Nicolas Papernot, Patrick McDaniel, Xi Wu, Somesh Jha, and Ananthram Swami. Distillation as a defense to adversarial perturbations against deep neural networks. In *2016 IEEE symposium on security and privacy (SP)*, pages 582–597. IEEE, 2016.
- [26] Andrew Ross and Finale Doshi-Velez. Improving the adversarial robustness and interpretability of deep neural networks by regularizing their input gradients. In *Proceedings of the AAAI Conference on Artificial Intelligence*, volume 32, 2018.
- [27] Anish Athalye, Nicholas Carlini, and David Wagner. Obfuscated gradients give a false sense of security: Circumventing defenses to adversarial examples. In *International Conference on Machine Learning*, pages 274–283. PMLR, 2018.
- [28] Gavin Weiguang Ding, Yash Sharma, Kry Yik Chau Lui, and Ruitong Huang. Mma training: Direct input space margin maximization through adversarial training. *arXiv preprint arXiv:1812.02637*, 2018.
- [29] Jingfeng Zhang, Xilie Xu, Bo Han, Gang Niu, Lizhen Cui, Masashi Sugiyama, and Mohan Kankanhalli. Attacks which do not kill training make adversarial learning stronger. In *International Conference on Machine Learning*, pages 11278–11287. PMLR, 2020.
- [30] Jingfeng Zhang, Jianing Zhu, Gang Niu, Bo Han, Masashi Sugiyama, and Mohan Kankanhalli. Geometry-aware instance-reweighted adversarial training. *arXiv preprint arXiv:2010.01736*, 2020.
- [31] Ting Chen, Simon Kornblith, Mohammad Norouzi, and Geoffrey Hinton. A simple framework for contrastive learning of visual representations. In *International conference on machine learning*, pages 1597–1607. PMLR, 2020.
- [32] Alexander Kolesnikov, Xiaohua Zhai, and Lucas Beyer. Revisiting self-supervised visual representation learning. In *Proceedings of the IEEE/CVF Conference on Computer Vision and Pattern Recognition*, pages 1920–1929, 2019.
- [33] Longlong Jing and Yingli Tian. Self-supervised visual feature learning with deep neural networks: A survey. *IEEE Transactions on Pattern Analysis and Machine Intelligence*, 2020.
- [34] Carl Doersch, Abhinav Gupta, and Alexei A Efros. Unsupervised visual representation learning by context prediction. In *Proceedings of the IEEE international conference on computer vision*, pages 1422–1430, 2015.
- [35] Spyros Gidaris, Praveer Singh, and Nikos Komodakis. Unsupervised representation learning by predicting image rotations. *arXiv preprint arXiv:1803.07728*, 2018.
- [36] Prannay Khosla, Piotr Teterwak, Chen Wang, Aaron Sarna, Yonglong Tian, Phillip Isola, Aaron Maschinot, Ce Liu, and Dilip Krishnan. Supervised contrastive learning. *arXiv preprint arXiv:2004.11362*, 2020.
- [37] Yaodong Yu, Kwan Ho Ryan Chan, Chong You, Chaobing Song, and Yi Ma. Learning diverse and discriminative representations via the principle of maximal coding rate reduction. *Advances in Neural Information Processing Systems*, 33, 2020.

Supplementary Material

A ATFS Algorithm

The detailed training algorithm for ATFS is shown in Algorithm 1. Specifically, we first construct an ATG $\mathcal{G} = \{\mathcal{V}, \mathcal{E}^+, \mathcal{E}^-\}$ based on the full training set (Step 3). In each iteration of the training, we first sample a mini-batch \mathcal{B} (Step 6), and then generate adversarial samples using Projected Gradient Descent (PGD) for samples in the current batch \mathcal{B} (Step 7). Based on the clean samples $\{\mathbf{x}_i\}$ and their corresponding adversarial samples $\{\mathbf{x}'_i\}$ in this mini-batch, we extract the subgraph \mathcal{G}_B from \mathcal{G} which contains clean and adversarial samples as nodes and their corresponding links (Step 8). Given the subgraph \mathcal{G}_B , we can easily calculate its Feature Separability Loss and we minimize the objective in Eq. (2.5) with respect to the model parameters θ by gradient descent. The procedures from Step 6 to Step 10 will be repeated until convergence.

Algorithm 1 Adversarial Training with Feature Separability

- 1: **Input:** Training data $\mathcal{D} = \{(\mathbf{x}_i, y_i)\}_{i=1}^n$, learning rate γ , momentum m , weight decay w , number of epochs T , batch size b
 - 2: **Output:** An adversarially robust model f_θ
 - 3: Construct an ATG $\mathcal{G} = \{\mathcal{V}, \mathcal{E}^+, \mathcal{E}^-\}$;
 - 4: **for** epoch = 1, ..., T **do**
 - 5: **for** mini-batch = 1, ..., $\lceil \frac{n}{b} \rceil$ **do**
 - 6: Sample a mini-batch $\mathcal{B} = \{(\mathbf{x}_i, y_i)\}_{i=1}^b$ from \mathcal{D} ;
 - 7: Generate adversarial samples $\{x'_i\}$ for \mathcal{B} by PGD attack;
 - 8: Extract a subgraph from ATG for the mini-batch $\mathcal{G}_B = \{\mathcal{V}_B, \mathcal{E}_B^+, \mathcal{E}_B^-\}$;
 - 9: Update θ based on the objective function in Eq. (2.5) by gradient descent with momentum m and weight decay w ;
 - 10: **end for**
 - 11: **end for**
-

B Experiment Result on WRN-34

Table 4: Performance Comparison on CIFAR10 with WRN-34-10.

	Clean	FGSM	PGD-20(8/255)	CW _{inf} (8/255)	AA(8/255)
AT	87.20	63.47±0.07	46.84±0.03	47.48±0.03	44.04
TRADES (1/λ = 5.0)	85.23	66.19±0.03	53.87±0.00	52.50±0.03	52.40
TRADES (1/λ = 6.0)	84.92	66.85±0.04	55.34±0.03	53.81±0.03	53.08
SS-OOD	81.61	62.49±0.00	49.80±0.00	49.27±0.00	48.88
MART	83.62	67.15±0.03	56.35±0.00	52.69±0.03	51.69
AT + ATFS	85.27	68.00±0.00	56.00±0.00	51.10±0.00	51.60
TRADES + ATFS	85.17	66.68±0.05	56.24±0.00	54.01±0.01	53.42
MART + ATFS	84.64	68.3±0.00	58.78±0.00	53.25±0.00	52.69